**Journal of Ultrafine Grained and Nanostructured Materials**
https://jufgnsm.ut.ac.ir
Vol. 49, No.1, June 2016, pp. 1-10
Print ISSN: 2423-6845 Online ISSN: 2423-6837
DOI: 10.7508/jufgnsm.2016.01.01

# Numerical Investigation of Size and Structure Effect on Tensile Characteristics of Symmetric and Asymmetric CNTs

***Mahnaz Zakeri*[*1], Omid Basiri[1]***

[1]*Aerospace Engineering Department, K.N.Toosi University of Technology, Tehran, 16765-3381, Iran*

*Recieved: 29 August 2015; Accepted: 30 May 2016*
*Corresponding author email: m.zakeri@kntu.ac.ir*

**ABSTRACT**

In this research, the influence of structure on the tensile properties of single- walled carbon nanotubes (CNTs) is evaluated using molecular mechanics technique and finite element method. The effects of diameter, length and chiral angle on elastic modulus and Poisson's ratio of armchair, zigzag and chiral structures are investigated. To simulate the CNTs, a 3D FEM code is developed using the ANSYS commercial software. Considering the carbon-carbon covalent bonds as connecting load-carrying beam elements, and the atoms as joints of the elements, CNTs are simulated as space-frame structures. The atomic potentials are estimated using harmonic simple functions. The numerical results show that by increasing the diameter and length to a certain amount, the size effect on tensile behavior of modeled nanotubes is omitted. In fact, for nanotubes with diameter over 2 nm and length over 36.5 nm the chiral angle is the only effective factor on the tensile properties. Also, it is found that the structure has a little effect on the elasticity modulus, which is about 4%. However, Poisson's ratio can be affected significantly with chiral angle. Asymmetric structures with angles $\theta < 18^{\circ}$ show higher Poisson's ratio in comparison with the other structures, such that it can be 16% larger for little chirality CNTs than armchair.

***Keywords:*** *Chirality; Elasticity modulus; Equivalent continuum modeling; Poisson's ratio.*

## 1. Introduction

Carbon nanotubes have exciting physical and mechanical properties that cause extensive interest to understand their behavior after the first introduction in 1991[1]. Carbon nanotubes have high stiffness and low density. From mechanical viewpoint, carbon nanotubes are the stiffest material known; with about 100 times more stiffness than the metal, they only weighs one-six of the metal. These amazing features put more emphasis on studying mechanical properties of such structures under different loading conditions.

Because of high costs and difficulties of experimental methods, many researchers have tended to use computational techniques such as molecular dynamics simulation and continuum modeling techniques to analyze the mechanical behavior of CNTs. Equivalent continuum modeling (ECM) is one the leading techniques of continuum modeling which is used as an efficient method for studying nano-structures at large scale. ECM is comprised of molecular mechanics and finite element method (FEM); mainly deal with nanotube modeling methods using shell, truss, spring and beam elements. ECM with shell elements was introduced by Yakobson et al. [2]. Odegard et al. [3] used ECM to find the relation between mechanics of solid and computational chemistry. Carbon nanotube bonds were replaced by truss elements and computational chemistry and continuum mechanics were interconnected by equalizing nanotube molecular potential energy and strain energy of the whole structure.

Li and Chou [4] introduced an FEM technique by replacing carbon-carbon bonds with representative beam elements. The beam element was defined based on the relation between molecular mechanics and continuum mechanics. They obtained Young's modulus of armchair and zigzag nanotubes at the range of 0.995 to 1.033 TPa, which was in good consistency with elastic modulus of graphene sheet. Xiao et al. [5] developed the FEM of beam elements using modified Morse potential. A similar method was used by Ávila and Lacerda [6], and they obtained elastic modules of CNTs at the range of 0.97 and 1.03 TPa. In addition, they reported that for nanotubes with small diameter, Young's modulus increases along with increase in the diameter.

The ECM and replacement of beam elements for carbon-carbon bonds was also used by Tserpes and Papanikos [7] and they concluded that chiral nanotubes have higher Young's modulus comparing with armchair and zigzag ones. In another research, Zaeri et al. [8] reported that armchair structure has higher Young's modulus comparing with zigzag structure. But, with increase of diameter, Young's modulus for the both structures is equal to 1.04 TPa. Shokrieh and Rafiee [9] employed the ECM to simulate armchair and zigzag nanotubes. They reported higher Young's modulus of armchair nanotubes than zigzag ones. Moreover, Lu and Hu [10] used ECM to compute the mechanical properties of carbon nanotubes. Their results showed increase of elastic modulus of zigzag and chiral CNTs with increase in diameter. However, only negligible changes on Young's modulus were observed for armchair structures.

Despite many studies published on mechanical properties of carbon nanotubes, the only covered area is the armchair, zigzag, and a few of chiral structures with certain angles. Indeed, there is not a comprehensive evaluation on the influence of structure on the CNT's properties. Since the chirality defines the engineering properties of CNTs, characterizing the tensile properties of chiral structures is a key to discover the science behind the tensile behavior of this kind of nanotubes, and understanding their capabilities for practical applications. The main goal of this study is to find out the role of nanotube structure on its mechanical properties. To this end, single walled CNTs of different structures (armchair, zigzag, and chiral) are simulated using ECM technique through replacing carbon-carbon bonds by the representative beam elements. Then, their tensile behavior is investigated through numerical analysis for different length, diameter, and chiral angles.

## 2. Atomic Structure of a Carbon Nanotube

A single-walled carbon nanotube can be simulated as a cylinder by rolling graphene sheet. The sheet is rolled along a specific vector known as chiral vector $\boldsymbol{C_h}$ defined as:

$$C_h = n\boldsymbol{a}_1 + m\boldsymbol{a}_2 \quad (1)$$

where $\boldsymbol{a}_1$ and $\boldsymbol{a}_2$ are unit vectors in the honeycomb lattice (figure 1) and the integer ordered pair of $(n,m)$ introduces the chiral index. Using $m$ and $n$, chiral angle $\theta$ can be determined based on Eq. 2:

$$\tan(\theta) = \frac{\sqrt{3}\,m}{2n+m} \quad (2)$$

Nanotubes with $(n,n)$ structure and chiral angle of 30° are known as armchair, and $(n,0)$ structures with chiral angle of 0° are known as zigzag. Also, CNTs with $(n,m)$ structures where $n>m$ and chiral angle of $0<\theta<30$ are known as chiral nanotubes. Diameter of nanotube ($D$) is obtained using Eq. 3 [11]:

$$D = \frac{a_{c-c}\sqrt{3\left(n^2+m^2+nm\right)}}{\pi} \quad (3)$$

in which, $a_{c-c}$ is the distance between two adjacent atoms (≅0.142 nm).

## 3. Principles of Molecular Mechanics

Molecular mechanics technique uses classical physic laws for predicting the molecular and structural properties. In molecular scale, interaction between the atoms is explained using potential energies of the molecules. Different methods and relations have been introduced to express the potential energies between the molecules such as Morse potentials, Tersoff-Brenner, and harmonics types [13]. These potentials provide different levels of accuracy for different applications. Although CNT structures show nonlinear behavior, the potential of bonds of molecular lattices with small deformations may be estimated using harmonic simple functions with acceptable accuracy. Based

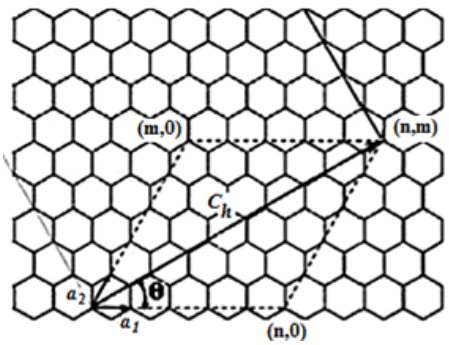


Fig. 1- Graphene sheet and parameters required to define nanotube structures [12].

on harmonic functions, different types of inter-atomic potential energy for covalent bonds of carbon atoms can be represented in the form of Eqs. 4-6 [14]:

$$U_r = \frac{1}{2}k_r(\Delta r)^2 \quad (4)$$

$$U_r = \frac{1}{2}k_r(\Delta r)^2 \quad (5)$$

$$U_\phi = \frac{1}{2}k_\phi(\Delta \phi)^2 \quad (6)$$

where $U_r$, $U_\theta$, and $U_\phi$ are the bond energies including bond stretching, bending, and torsion respectively; and $\Delta r$, $\Delta\theta$, $\Delta\phi$ represent variations in length, in-plane angle, and out of plane twist angle of the bond. Also, $k_r$, $k_\theta$, and $k_\phi$ are the force constants of bond stretching, bending, and torsion respectively. These constants are listed in Table 1 based on the results presented by Cornell et al. [15]. In this reference, $k_r$ and $k_\theta$ values have been used as starting values adjusted as necessary to reproduce experimental normal mode frequencies. These values were initially derived by fitting to structural and vibrational frequency data on small molecular fragments making up proteins and nucleic acids. For example, in complex fragments such as the nucleic acid bases, the $k_r$ values determined by linear interpolation between pure single and double bond values using the observed bond distances and the $k_\theta$ value taken from vibrational analysis of a simple $sp^2$ atom containing fragments such as benzene. Finally, for $k_r$, $k_\theta$, and $k_\phi$ constants the values of 938, 126, and 40 kcal $mole^{-1}A^{0-2}$ have been derived. In 2005, Tserpes and Papanikos [7] used the results from Ref. [15] to adopt the values of $k_r$, $k_\theta$, and $k_\phi$ according to Table 1.

Table 1- Force constants of molecular harmonic potential [7]

| Force constants | Quantity |
|---|---|
| $k_r$ | $652\left(\frac{\text{nN}}{\text{nm}}\right)$ |
| $k_\theta$ | $0.876\left(\frac{\text{nN.nm}}{\text{Rad}^2}\right)$ |
| $k_\phi$ | $0.278\left(\frac{\text{nN.nm}}{\text{Rad}^2}\right)$ |

## 4. Finite Element Modeling

As mentioned earlier, equivalent continuum modeling is comprised of molecular mechanics and FEM methods. The equality of inter-molecular potential energy in chemistry and strain energy in structural mechanics was ensured by Li and Chou [4]. Given that covalent bonds act as connecting elements of carbon atoms in the molecular lattice, carbon-carbon bond may be taken as a beam in structure where the atoms act as connection of the bonds. Li and Chou [4] drawn a direct relation between structural mechanic properties $E_oA_o$, $E_oI_o$, and $G_oJ_o$ and parameters of molecular mechanics $k_r$, $k_\theta$, and $k_\phi$ (Eq. 7):

$$k_r = \frac{E_oA_o}{L_o}, \quad k_\theta = \frac{E_oI_o}{L_o}, \quad k_\phi = \frac{G_oJ_o}{L_o} \quad (7)$$

where, $L_o$, $A_o$, $I_o$, $J_o$, $E_o$, and $G_o$ are length, cross sectional area, moment of inertia, polar moment of inertia, elastic modulus, and shear modulus, respectively of a beam element with a circular cross section of diameter *d*. Then, cross-sectional area, moment of inertia, and polar moment of inertia of beam element are:

Length of the replaced beam element is equal with the length of carbon-carbon bond. By replacing Eq. 8 in Eq. 7 and using the specific values of potential energy coefficients (Table 1), diameter, elastic modulus, and shear modulus of the beam element are obtained. Having the diameter, area of cross-section, and moment of inertia of the replaced beam element can be obtained using Eq. 8 (Table 2).

$$A_o = \frac{\pi d^2}{4}, \quad I_o = \frac{\pi d^4}{64}, \quad J_o = \frac{\pi d^4}{32} \quad (8)$$

Table 2- Geometric and mechanical properties of the beam element used in FEM

| Parameter | Quantity |
|---|---|
| Bond/beam length ($L_o$) | 0.142 nm |
| Diameter ($d$) | 0.1466 nm |
| Cross section area ($A_o$) | 0.0169 $nm^2$ |
| Moment of inertia ($I_o$) | $2.27\times10^{-5}$ $nm^4$ |
| Elastic modulus ($E_o$) | 5.4836 TPa |
| Shear modulus ($G_o$) | 0.8701 TPa |

By determining coordinates of carbon atoms (nodes) and using a simple algorithm, geometric model of different kinds of carbon nanotubes was obtained. Afterward, position matrix for each element was developed between the corresponding two nodes and having the stiffness matrix of each element and inducing loading and boundary condition, FEM of the carbon nanotubes was obtained for different length and diameters.

Since CNTs carbon atoms are bonded together with covalent bonds having a characteristic bond length $a_{C-C}$ and bond angle in the 3D space, the displacement of each atom under an external force is constrained by the bonds, and the total deformation of nanotube is the result of interactions between the bonds. As mentioned by Tserpes and Papanikos [7], considering the bonds as connecting load-carrying beam elements, and the atoms as joints of the elements, CNTs could be simulated as space-frame structures. By treating CNTs as space-frame structures, their mechanical behavior can be analyzed using classical structural mechanics methods. A schematic of beam element replacement with carbon-carbon bond, to be used in FEM, is illustrated in figure 2.

In this research, a 3D FEM code is developed using the ANSYS commercial software. For the modeling of the bonds, the 3D elastic BEAM 188 element is used which is a uni-axial element with tension, compression, torsion and bending capabilities. It has six degrees of freedom at each node; including translations and rotations about the nodal x, y, and z-axes. Geometric and mechanical properties of the element are defined according to Table 2. Figure 3 shows finite element model of three types of nanotubes.

## 5. Tensile Properties of Carbon Nanotubes

### 5.1. Young's Modulus

To compute the mechanical properties, first proper boundary condition and loading should be implemented. In computation of Young's modulus of single-walled carbon nanotubes, all degrees of freedom of nodes are closed at the end of nanotube

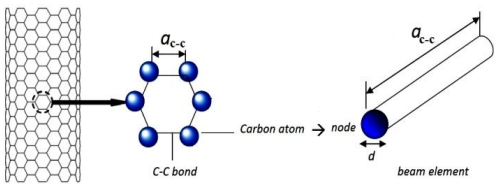


Fig. 2. Replacement of beam element with C-C bonds in CNT [16].

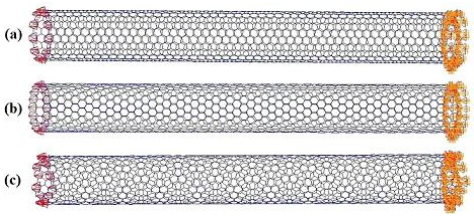


Fig. 3. Finite element model of CNTs: a) armchair (11,11), b) zigzag (18,0), c) chiral (14,7).

and a small displacement equal to 1% strain is induced to the nodes at the tip of the nanotube (Fig.3). Having the displacement implemented, total axial forces on the nodes located at the end of the nanotube were calculated by software. Then, Young's modulus of carbon nanotubes under tension is obtained using Eq. 9.

$$E = \frac{F\,L}{\Delta L\;A} \tag{9}$$

where, $F$, $L$, $\Delta L$, and $A$ represent the total implemented axial forces at the end of nanotube, length, change of length, and cross sectional area of the nanotube, respectively. To calculate the cross-sectional area, the carbon nanotube is considered as a continuous tube with a thickness equal to Van der Waals diameter of carbon atom which is 0.34 nm [17].

### 5.2. Poisson's Ratio

Based on classic theory of elasticity, Poisson's ratio of CNTs ($n$) is obtained using Eq. 10.

$$\nu = -\frac{\varepsilon_{radial}}{\varepsilon_{axial}} = -\frac{\Delta R/R}{\Delta L/L} \tag{10}$$

where, $\varepsilon_{radial}$ is radial strain, $\varepsilon_{axial}$ is axial strain, $\Delta L$ is change of length (i.e. induced displacement of the nodes at the tip of nanotube), $\Delta R$ is radius change, $R$ is radius, and $L$ is length of the nanotube.

## 6. Results and Discussion

The mechanical behavior of CNTs can be influenced by their geometry. Hence, the influence of geometrical parameters of diameter, length, and chiral angle on Young's modulus and Poisson's ratio should be studied separately to recognize the roll of chirality. In the following, tensile properties obtained by numerical analyses of CNTs are presented.

### 6.1. Effect of Nanotube Diameter

Many researchers have been engaged in investigating the effect of diameter on Young's modulus of carbon nanotubes. However, the main

body of the literature has only focused on armchair and zigzag structures. In this work, all three structures of CNTs (armchair, zigzag, and chiral) are studied. To find the effect of diameter on CNT's tensile behavior, nanotubes with the same length and chiral angle must be analyzed. Therefore, in this step, armchair, zigzag, and chiral structures with constant chiral angle of 19.11° are modeled such that all CNTs of these three structural groups have the lengths of 12.6665, 12.638, and 12.6664 nm, respectively. Table 3 presents the geometrical characteristics of the studied armchair, zigzag, and chiral nanotubes with different diameters. After calculating Young's modulus using Eq. 9, the effect of diameter on this parameter is obtained and plotted according to figure 4.

As shown in figure 4, increase in diameter for all types of structures with small diameter results in increase of Young's modulus. However, the increase is trivial and almost zero for diameters more than 2 nm. The effect of curvature in carbon-carbon bonds was mentioned by Li and Chou [4] as the reason of the increase in Young's module for CNTs with small diameter. In fact, nanotubes with small diameters have larger curvature than those with larger diameter which means higher distortion of c-c bonds in nanotubes with small diameter. This curvature decreases with increase of diameter; and Young's modulus of nanotubes approaches to Young's modulus of graphene sheet. It should be mentioned that there are some size effects such as nonlocal effect of the interatomic interaction; which did not considered in the present study because of using the simple laws to calculate the atomic potentials. A more accurate model could be derived when accounting for the long-range interaction.

To ensure removal of the diameter effect, the diameters of the nanotubes have been investigated up to 5 nm. As pictured in figure 4, chiral nanotube of angle $\theta$ =19.11° has higher Young's modulus than armchair and zigzag nanotubes; and zigzag has the smallest Young's modulus.

To evaluate the validity of current FEM modeling and results, Young's modulus for armchair nanotubes with (5,5) and (15,15) structures, zigzag nanotubes with (9, 0) and (21, 0) structures, and chiral nanotubes with (8,4) and (16, 8) structures are compared with the results presented in Refs. [4,8,10] in Table 4. Moreover, a comparison between Young's modulus obtained in this study and that of other works with similar diameter range is shown in Table 5. A considerable consistency between the results is evident.

At the next step, Poisson's ratio ($n$) was determined using Eq. 10 and variation diagram was plotted against the diameter of nanotube. Figure 5 illustrates the effect of diameter on Poisson's ratio. Clearly, this parameter increases with increase of diameter in armchair and chiral CNTs at small diameters, but zigzag structure has the maximum Poisson's ratio in small diameters, and increase in the diameter leads to decrease in $n$. However, the zigzag structure shows a behavior similar to the other structures for diameters over 1.644 nm.

These results show that armchair nanotube has the lowest Poisson's ratio. Furthermore, the studied chiral nanotubes ($\theta$ =19.11°) has higher Poisson's ratio than symmetric structures of zigzag and armchair for diameters below 1.2 nm; and for diameters over 2 nm, the effect of diameter on $n$ is negligible and this parameter can be considered constant.

For verification of the results, a comparison with the few available results from previous studies was made. The results presented by Lu [19] shows that Poisson's ratio for CNTs with diameters over 1 nm is between 0.26 and 0.32. On the other hand, Sun and Zhao [20] reported that $n$ is 0.31 for armchair nanotube with diameter of 2.8 nm. In the present work, Poisson's ratio for armchair nanotube of (21, 21) with a diameter of 2.8 nm is equal to 0.3096 which is consistent with Ref. [20]. Also, Poisson's ratio for zigzag and armchair carbon nanotubes was examined by Natsuki et al. [21] through modeling the CNTs using spring elements; in addition to an analytical method. According to their results, Poisson's ratio for armchair and zigzag nanotubes with diameters at the range of 0.5-2.5 nm was obtained as 0.27-0.29 and 0.27-0.33, respectively

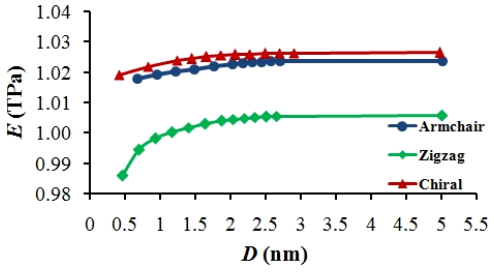


Fig. 4- Variation of Young's modulus versus diameter of nanotubes.

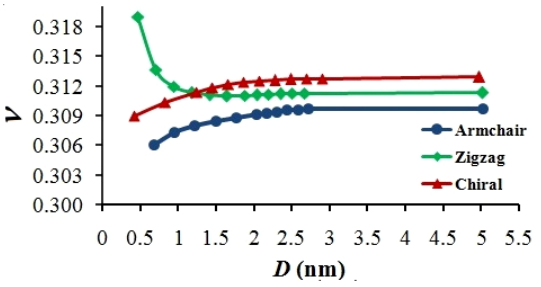


Fig. 5- Variation of Poisson's ratio versus diameter of nanotube.

Table 3- Geometrical characteristics of simulated nanotubes for investigating the effect of diameter

| Structure | $(n,m)$ | Chirality($\theta^\circ$) | Diameter (nm) | Length (nm) | Nodes | Elements |
|---|---|---|---|---|---|---|
| Armchair | (5,5) | 30 | 0.6780 | 12.6665 | 1040 | 1550 |
| | (7,7) | 30 | 0.9492 | 12.6665 | 1456 | 2170 |
| | (9,9) | 30 | 1.2204 | 12.6665 | 1872 | 2790 |
| | (11,11) | 30 | 1.4916 | 12.6665 | 2288 | 3410 |
| | (13,13) | 30 | 1.7628 | 12.6665 | 2704 | 4030 |
| | (15,15) | 30 | 2.0340 | 12.6665 | 3120 | 4650 |
| | (16,16) | 30 | 2.1696 | 12.6665 | 3328 | 4960 |
| | (17,17) | 30 | 2.3052 | 12.6665 | 3536 | 5270 |
| | (18,18) | 30 | 2.4408 | 12.6665 | 3744 | 5580 |
| | (19,19) | 30 | 2.5764 | 12.6665 | 3952 | 5890 |
| | (20,20) | 30 | 2.7120 | 12.6665 | 4160 | 6200 |
| | (37,37) | 30 | 5.0172 | 12.6665 | 7696 | 11470 |
| Zigzag | (6,0) | 0 | 0.4697 | 12.6380 | 720 | 1074 |
| | (9,0) | 0 | 0.7046 | 12.6380 | 1080 | 1611 |
| | (12,0) | 0 | 0.9395 | 12.6380 | 1440 | 2148 |
| | (15,0) | 0 | 1.1743 | 12.6380 | 1800 | 2685 |
| | (18,0) | 0 | 1.4092 | 12.6380 | 2160 | 3222 |
| | (21,0) | 0 | 1.6441 | 12.6380 | 2520 | 3759 |
| | (24,0) | 0 | 1.8789 | 12.6380 | 2880 | 4296 |
| | (26,0) | 0 | 2.0355 | 12.6380 | 3120 | 4654 |

| | | | | | | |
|---|---|---|---|---|---|---|
| | (28,0) | 0 | 2.1921 | 12.6380 | 3360 | 5012 |
| | (30,0) | 0 | 2.3487 | 12.6380 | 3600 | 5370 |
| | (32,0) | 0 | 2.5052 | 12.6380 | 3840 | 5728 |
| | (34,0) | 0 | 2.6618 | 12.6380 | 4080 | 6086 |
| | (64,0) | 0 | 5.0105 | 12.6380 | 7680 | 11456 |
| Chiral | (4,2) | 19.11 | 0.4143 | 12.6664 | 630 | 939 |
| | (8,4) | 19.11 | 0.8285 | 12.6664 | 1262 | 1881 |
| | (12,6) | 19.11 | 1.2428 | 12.6664 | 1894 | 2823 |
| | (14,7) | 19.11 | 1.4499 | 12.6664 | 2198 | 3276 |
| | (16,8) | 19.11 | 1.6571 | 12.6664 | 2526 | 3765 |
| | (18,9) | 19.11 | 1.8642 | 12.6664 | 2842 | 4236 |
| | (20,10) | 19.11 | 2.0713 | 12.6664 | 3140 | 4680 |
| | (22,11) | 19.11 | 2.2785 | 12.6664 | 3454 | 5148 |
| | (24,12) | 19.11 | 2.4856 | 12.6664 | 3790 | 5649 |
| | (26,13) | 19.11 | 2.6927 | 12.6664 | 4106 | 6120 |
| | (28,14) | 19.11 | 2.8999 | 12.6664 | 4396 | 6552 |
| | (48,24) | 19.11 | 4.9712 | 12.6664 | 7582 | 11301 |

[21]. They reported that Poisson's ratio for zigzag structure is higher than that of armchairs, which is consistent with the present results.

**6.2. Effect of nanotube length**

To study the effect of nanotube length on its tensile properties, it is needed to model the CNTs with the same diameter. For this aim, armchair (15, 15), zigzag (26, 0), and chiral (21, 8) with chiral angle of 15.49° with fixed diameters of 2.034, 2.035, and 2.031 nm (respectively) are simulated. The length of the modeled CNTs is varying at the range of 6-61 nm. The obtained results for Young's modulus and Poisson's ratio are illustrated in Figs. 6 and 7.

As illustrated in Figs. 6 and 7, increase in the length results in reduction of Young's modulus and Poisson's ratio for all three types of nanotube. However, for lengths more than 36.5 nm, the changes are almost trivial and these mechanical properties are almost constant. Changes in the mechanical properties with increasing the length from 36.5nm to 61nm are very little (<1%), indicating that tensile properties are not dependent

Table 4- Comparison of results for Young's modulus obtained in this work and previous studies for different structures of CNTs

| SWCNT | Young's modulus , $E$ (TPa) | | | |
|---|---|---|---|---|
| $(n,m)$ | Li and Chou [4] | Zaeri et al. [8] | Lu and Hu [10] | Present work |
| (5,5) | 0.99 | 1.038 | 1.016 | 1.018 |
| (15,15) | 1.02 | 1.04 | 1.015 | 1.0226 |
| (9,0) | 0.995 | 1.015 | - | 0.994 |
| (21,0) | 1.028 | 1.037 | - | 1.003 |
| (8,4) | - | 0.966 | 1.015 | 1.022 |
| (16,8) | - | 0.97 | 1.031 | 1.025 |

Table 5- Comparison of results for Young's modulus obtained in this work and previous studies for CNTs with similar diameter range

| Researchers | CNT diameter (nm) | $E$ (TPa) |
|---|---|---|
| Li and Chou [4] | 0.391- 2.035 | 0.891- 1.036 |
| Ávila and Lacerda [6] | 0.391- 1.801 | 0.978- 1.033 |
| Zaeri et al. [8] | 0.391- 2.071 | 0.935- 1.04 |
| Lu and Hu [10] | 0.391- 2.071 | 0.989- 1.058 |
| Yang et al. [18] | 0.678 | 1.03 |
| Present work | 0.414- 2.071 | 0.986- 1.026 |

to the length for nanotubes with length over 36.5 nm.

According to the results, chiral nanotube has the highest Young's modulus and Poisson's ratio in comparison with the other structures; and zigzag structure has the lowest Young's modulus among all. Moreover, armchair structure has the lowest Poisson's ratio. To achieve deeper insight on the roll of CNT structure on its tensile properties, in the following section, the effect of chiral angle is taken into account apart from the influence of nanotube size.

### 6.3. Effect of chiral angle

In the previous sections, it was mentioned that the size effects on tensile properties vanish for nanotubes with diameter over 2 nm and length over 36.5 nm. Consequently, the only parameter affecting the mechanical properties of such nanotubes is the chiral angle. In this step, the effect of chirality on mechanical properties is studied for different kinds of CNTs with diameter and length over 2 nm and 36.5 nm, respectively. The characteristic of the modeled nanotubes are presented in Table 6.

Figs. 8 and 9 illustrate the variation of Young's modulus and Poisson's ratio against chiral angle,

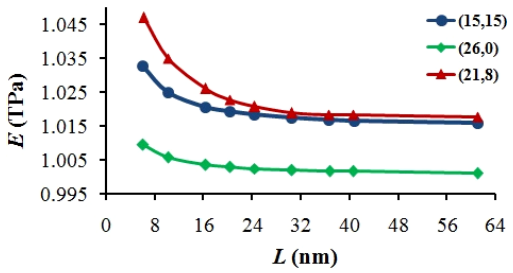


Fig. 6- Variation of Young's modulus versus length of nanotube.

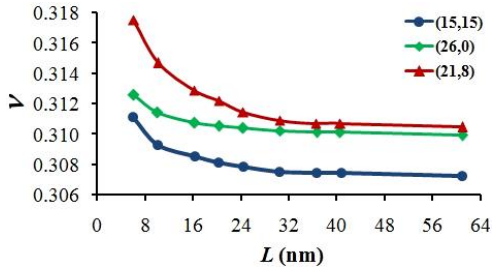


Fig. 7- Variation of Poisson's ratio versus length of nanotube.

Table 6- Characteristics of CNTs simulated for analyzing the effect of chiral angle

| (*n*,*m*) | Chirality ($\theta^\circ$) | Diameter (nm) | Length (nm) | Nodes | Elements |
|---|---|---|---|---|---|
| (26,0) | 0 | 2.0355 | 36.7070 | 8996 | 13468 |
| (26,1) | 1.87 | 2.0758 | 36.6553 | 9105 | 13642 |
| (25,2) | 3.81 | 2.0400 | 36.7157 | 8970 | 13428 |
| (24,4) | 7.59 | 2.0535 | 36.6941 | 9026 | 13511 |
| (23,6) | 11.30 | 2.0758 | 36.7021 | 9128 | 13663 |
| (21,8) | 15.49 | 2.0310 | 36.5561 | 8898 | 13318 |
| (20,10) | 19.11 | 2.0713 | 36.6573 | 9102 | 13623 |
| (18,12) | 23.41 | 2.0475 | 36.6166 | 9000 | 13470 |
| (16,14) | 27.80 | 2.0355 | 36.6251 | 8942 | 13383 |
| (15,15) | 30 | 2.0340 | 36.6467 | 8970 | 13425 |

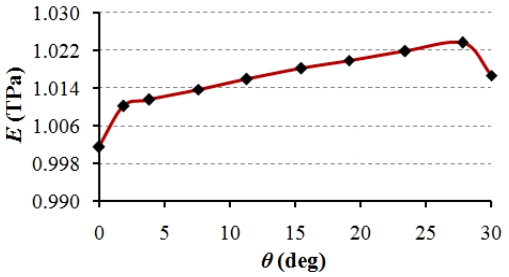


Fig. 8. Variation of Young's modulus versus chiral angle.

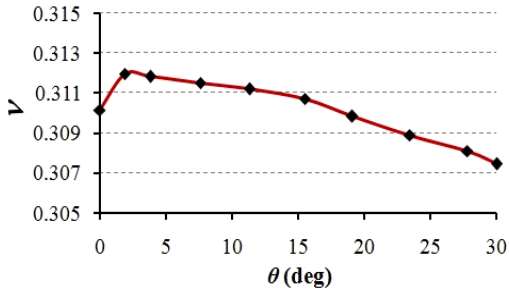


Fig. 9. Variation of Poisson's ratio versus chiral angle.

respectively. As shown in figure 8, zigzag structure has the smallest Young's modulus comparing with the other structures. Increase of chiral angle leads to increase of Young's modulus in chiral structures. Chiral nanotubes with angle $\theta$ <13° have smaller Young's modulus than armchair structure, while for angles $\theta$ >13° chiral nanotubes have the higher Young's modulus comparing with the other structures.

About Poisson's ratio, as shown in figure 9, the armchair nanotube has the lowest *n*. Also, increase in chiral angle leads to decrease of Poisson's ratio in chiral structures. In addition, comparing with the symmetric structures, highest *n* is achieved for chiral structures with angle less than 18°.

## 7. Conclusion

In this paper, tensile properties of different types of carbon nanotube were studied using molecular mechanics and FEM techniques. Young's modulus and Poisson's ratio were obtained for carbon nanotubes of a wide range of diameters and lengths. Examination of relation between the mechanical properties and diameter and length of CNTs revealed that with increasing of diameter and length over a specific amount, the size effect on Young's modulus and Poisson's ratio will be eliminated. According to the results, for nanotubes with diameter over 2 nm and length over 36.5 nm, the chiral angle is the only effective factor on tensile properties. Regarding such nanotubes, the results show that zigzag structure has the lowest Young's

modulus comparing with armchair and chiral structures, and chiral nanotubes with angle $\theta$ >13° have higher Young's modulus in comparing with the other structures.

Concerning Poisson's ratio, it is found that armchair structure has the lowest Poisson's ratio comparing with the two other structures. Moreover, chiral structures with angles $\theta$ <18° showed higher Poisson's ratio in comparison with the other structures; so that for little angles (about 2°), Poisson's ratio is considerably larger (more than 16%) than armchair structure.

## References


1. Iijima S. Helical microtubules of graphitic carbon. nature. 1991;354(6348):56-8.
2. Yakobson BI, Brabec CJ, Bernholc J. Nanomechanics of carbon tubes: instabilities beyond linear response. Physical review letters. 1996;76(14):2511.
3. Odegard GM, Gates TS, Nicholson LM, Wise KE. Equivalent-continuum modeling of nano-structured materials. Composites Science and Technology. 2002;62(14):1869-80.
4. Li C, Chou TW. A structural mechanics approach for the analysis of carbon nanotubes. International Journal of Solids and Structures. 2003;40(10):2487-99.
5. Xiao JR, Gama BA, Gillespie JW. An analytical molecular structural mechanics model for the mechanical properties of carbon nanotubes. International Journal of Solids and Structures. 2005;42(11):3075-92.
6. Ávila AF, Lacerda GS. Molecular mechanics applied to single-walled carbon nanotubes. Materials Research. 2008;11(3):325-33.
7. Tserpes KI, Papanikos P. Finite element modeling of single-walled carbon nanotubes. Composites Part B: Engineering. 2005;36(5):468-77.
8. Zaeri MM, Ziaei-Rad S, Vahedi A, Karimzadeh F. Mechanical modelling of carbon nanomaterials from nanotubes to buckypaper. Carbon. 2010;48(13):3916-30.
9. Shokrieh MM, Rafiee R. Prediction of Young's modulus of graphene sheets and carbon nanotubes using nanoscale continuum mechanics approach. Materials & Design. 2010;31(2):790-5.
10. Lu X, Hu Z. Mechanical property evaluation of single-walled carbon nanotubes by finite element modeling. Composites Part B: Engineering. 2012;43(4):1902-13.
11. Gogotsi Y, editor. Nanomaterials handbook. CRC press; 2006.
12. Kalamkarov AL, Georgiades AV, Rokkam SK, Veedu VP, Ghasemi-Nejhad MN. Analytical and numerical techniques to predict carbon nanotubes properties. International journal of Solids and Structures. 2006;43(22):6832-54.
13. Rafii-Tabar H. Computational modelling of thermo-mechanical and transport properties of carbon nanotubes. Physics Reports. 2004;390(4):235-452.
14. Gelin BR. Molecular modeling of polymer structures and properties. Hanser Publishers; Hanser/Gardner Publications; 1994.
15. Cornell WD, Cieplak P, Bayly CI, Gould IR, Merz KM, Ferguson DM, Spellmeyer DC, Fox T, Caldwell JW, Kollman PA. A second generation force field for the simulation of proteins, nucleic acids, and organic molecules. Journal of the American Chemical Society. 1995;117(19):5179-97.
16. Gaddamanugu D. M.Sc. Thesis. Texas A & M University.2009.
17. Giannopoulos GI, Kakavas PA, Anifantis NK. Evaluation of the effective mechanical properties of single walled carbon nanotubes using a spring based finite element approach. Computational Materials Science. 2008;41(4):561-9.
18. Yang QS, Li BQ, He XQ, Mai YW. Modeling the mechanical properties of functionalized carbon nanotubes and their composites: design at the atomic level. Advances in Condensed Matter Physics. 2014;482056;doi: 10.1155/2014/482056.
19. Lu JP. Elastic properties of carbon nanotubes and nanoropes. Physical Review Letters. 1997;79(7):1297.
20. Sun X, Zhao W. Prediction of stiffness and strength of single-walled carbon nanotubes by molecular-mechanics based finite element approach. Materials Science and Engineering: A. 2005;390(1):366-71.
21. Natsuki T, Tantrakarn K, Endo M. Effects of carbon nanotube structures on mechanical properties. Applied Physics A. 2004;79(1):117-24.